JMEPEG (2018) 27:3199–3205
https://doi.org/10.1007/s11665-018-3433-4

1059-9495/$19.00

Microstructure and Mechanical Properties of a Ag Micro-Alloyed Mg-5Sn Alloy

S.H. Huang

(Submitted October 13, 2017; in revised form March 17, 2018; published online May 29, 2018)

Effects of 1.5 wt.% Ag addition and solid solution + artificial ageing at 160 °C on the microstructure and mechanical properties of a Mg-5Sn alloy have been studied. The results show that Ag addition has significantly hardened the solution-treated Mg-5Sn alloy. During the ageing process, the hardness increase rate and the strength and ductility of the Mg-5Sn alloy at each state are also improved by Ag addition. The improved strengthening behavior is primarily attributed to the refinement distribution of the Mg_2Sn precipitates, the enhanced precipitation process, and the synergistic strengthening effect of Mg_2Sn and a metastable plate DO_{19} phase formed at lower ageing temperature. For each solution-treated alloy, the strength and ductility are higher than the corresponding cast ones. Ageing further enhances the yield strength, and the ductility of the Mg-5Sn-1.5Ag alloy is also increased after ageing. The fracture surfaces of the both peak-aged alloys exhibit the characteristic of a mixture of quasi-cleavage and ductile fracture.

Keywords age hardening, Mg-Sn alloy, micro-alloying, precipitation, tensile properties

1. Introduction

Among various strengthening methods of alloys, precipitation strengthening is an effective and practical way for many Mg alloys. The major alloying elements of Mg alloys such as Al, Zn, RE, and Sn all have a large solid solubility in Mg matrix, and the solubility decreases considerably with decrease of the temperature (Ref 1), which provides a good condition for the precipitation strengthening. The detailed precipitation sequence and crystallographic features of the precipitates in these typical age-hardening Mg alloys have been well summarized in recent reviews (Ref 2, 3). Mg-Sn alloys is one group of the typical precipitation-strengthening alloys which have good potential for application in elevated temperature conditions due to the high melting point of the Mg_2Sn precipitates and the high eutectic temperatures (Ref 4, 5). Therefore, Mg-Sn alloys have aroused considerable concern in recent years. In addition to their application in the cast state, Mg-Sn alloys also have great potential for use as wrought alloys (Ref 6-8). A common way to strengthen wrought alloys is artificial ageing treatment after deformation of the solid-solution-treated alloys. In order to improve the age-hardening response of Mg-Sn alloys, various micro-alloying elements have been added to the alloy, and a good enhancing effect has been obtained (Ref 9-13). Ag is one of the effective micro-alloying elements because it can form solute clusters before the precipitation of Mg_2Sn, thus acting as an effective heterogeneous nucleation sites for the precipitates. As a result, the Mg_2Sn precipitates can be refined significantly and the strengthening effect is improved remarkably (Ref 14).

Usually, artificial ageing treatment of most Mg alloys is conducted at 200 °C. It was initially believed that the precipitation sequence of Mg-Sn alloys during ageing treatment did not involve the formation of any metastable phases (Ref 3). The major role of the micro-alloying elements was found to refine the distribution of the Mg_2Sn phases, leading to an enhanced ageing response (Ref 9, 10, 14). In a recent study, however, a metastable DO_{19} phase has been observed in an aged Mg-1.5at.%Sn alloy with an ageing temperature of 150 °C (Ref 15). Though the time needed to reach peak ageing was delayed, the peak hardness could be significantly improved at lower ageing temperature (Ref 15). More recently, Liu et al. (Ref 16) have further examined the precipitation sequence of an aged Mg-9.8wt.%Sn alloy using aberration-corrected scanning transmission electron microscopy (STEM), and they have found that a GP zone and a metastable phase were formed prior to the equilibrium Mg_2Sn phase. Considering the formation of the metastable phase, it provides us with a good idea to further improve the age-hardening response of Mg-Sn alloys by decreasing the ageing temperatures.

Recently, Huang et al. (Ref 11) have studied the effects of different micro-alloying Ag contents on the age-hardening response of a Mg-5wt.%Sn alloy. They found that the hardening response was improved proportionally with the Ag added. A peak-aged hardness value of a Mg-5Sn-2Ag alloy at 200 °C is 67.3HV (Ref 11). However, increasing the Ag content will certainly result in higher cost of the alloy. To further improve the age-hardening response and decrease the cost of the alloy, Mg-5Sn-1.5Ag alloys subjected to solid-solution and ageing treatment at 160 °C were developed in the present study. The aim of this study is to employ the formation of the metastable precipitates at lower ageing temperatures as well as the micro-alloying effects of Ag on refining the precipitates distributions. As a result, a reasonable age-hardening response of a Mg-Sn alloy with lower cost can be obtained. In addition, while most of the previous studies focused on the hardness of the Mg-Sn alloys during ageing treatment, the present work further investigated the strength and ductility of the Mg-5Sn-(1.5Ag) alloys at different states, and the relationship between the microstructure and the mechanical properties has also been discussed.

S.H. Huang, Southwest Technology and Engineering Research Institute, Chongqing 400039, China. Contact e-mail: hsh82@163.com.

2. Experimental Methods

Alloy ingots with nominal compositions of Mg-5Sn and Mg-5Sn-1.5Ag in weight percent were prepared in an electrical furnace under mixed atmospheres of CO_2 and SF_6 and then cast into a mild steel mold. Some of the cast samples were homogenized at 460 °C for 24 h and then solution-treated at 480 °C for 2 h, followed by quenching into cold water. To prevent oxidation, the alloy samples were buried in compacted carbon powder during homogenization and solid-solution treatment. Afterward, the solution-treated samples were artificially aged at 160 °C in a drying oven for different holding times. The age-hardening responses of the samples were measured by a Vickers hardness tester under a load of 1.96 N. Optical microscopy (OM) samples were prepared by mechanically grinding and polishing and then etched in a solution of acetic picral (2 ml of acetic acid, 2.5 g of picric acid, 4 ml of distilled water, and 40 ml of ethanol). Analysis of phase constituents of the alloys was carried out in a DX-2700 x-ray diffraction (XRD) device. Samples for transmission electron microscopy (TEM) characterization were prepared by a twin-jet electro-polishing unit with an electrolyte composed of 4% perchloric acid and 96% ethanol at − 40 °C, with the electro-polishing voltage and current being 50 V and 10 mA, respectively. TEM characterization was performed in a FEI G^2 F20 microscope operating at 200 kV.

Tensile specimens were cut into slices with an electrical discharge wire cutting at the middle of each sample. The gauge dimension of each specimen was 10 mm × 3 mm × 2.5 mm, and three samples of each alloy were used to obtain the averaged value of the mechanical properties. The tensile tests were conducted at room temperature and with a crosshead speed of 1 mm/min on an electro-universal tester (Instron5569). The fractured surfaces of the tensile samples were observed in a scanning electron microscope (SEM, S-3400N) to analyze the fracture mechanism of the alloys.

3. Results and Discussions

The OM microstructure of the cast and solution-treated alloys under investigation is shown in Fig. 1. It can be seen that both the cast Mg-5Sn and Mg-5Sn-1.5Ag alloys show a dendrite-like grain morphology. The cast alloys contain α-Mg grains and eutectic intermetallics along the grain boundaries. These eutectics probably result from the non-equilibrium solidification process. The average grain size of the both alloys is around 100 μm. After the solid-solution treatment, all the intermetallics along the grain boundaries disappeared, indicating that they were successfully dissolved into the matrix. Because of the relatively long holding time at the high temperature of homogenization and solid solution, the grain sizes clearly grew to be coarser. The average grain size of the both alloys at the solution state is around 150 μm. No obvious refining effect of Ag elements was detected.

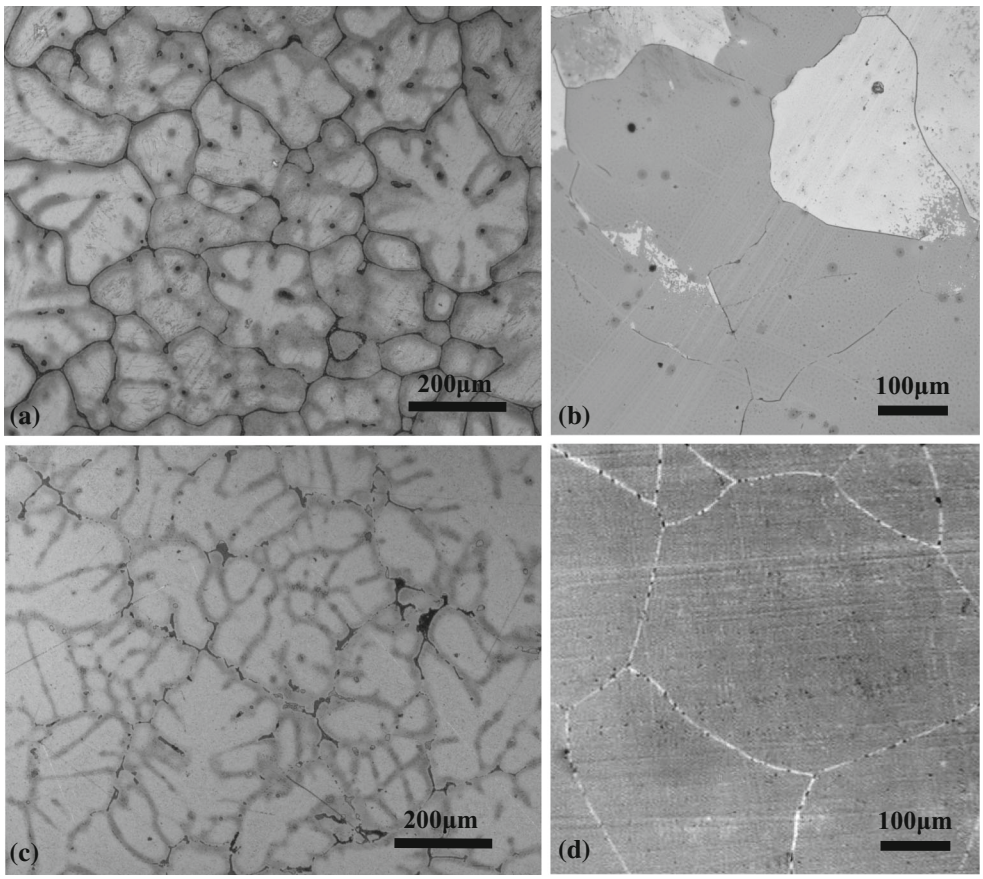

Fig. 1 OM microstructure of the investigated alloys. (a) As-cast Mg-5Sn alloy, (b) solution-treated Mg-5Sn alloy, (c) as-cast Mg-5Sn-1.5Ag alloy, and (d) solution-treated Mg-5Sn-1.5Ag alloy

Figure 2 shows the age-hardening response of the solid-solution-treated Mg-5Sn and Mg-5Sn-1.5Ag alloys. The hardness value of the solid-solution-treated Mg-5Sn alloys is about 50HV. During the ageing process at 160 °C, a clear hardness drop at the initial ageing stage of the Mg-5Sn alloy could be observed. Similar phenomenon was also reported in the ageing process of Mg-5Sn alloys at 200 °C in previous studies (Ref 11). Then, during the long-time ageing, both the increase and decrease in the hardness could be observed. This fluctuation was maintained until the ageing time reached 120 h, when the Mg-5Sn alloy still had a hardness of 50HV. Then, the hardness started to increase steadily. The peak hardness value of about 54HV of the Mg-5Sn alloy was obtained after 240 h ageing. During the overageing stage, the hardness decreased quickly to about 48HV at the 400th hour ageing. Later, the hardness value almost remained constant until 1000 h of ageing. The solution-treated Mg-5Sn-1.5Ag alloy had a hardness of 61HV. This is remarkably higher than that of the solution-treated Mg-5Sn alloy, indicating the significantly improved solid-solution strengthening effects of Ag addition. During the ageing process, similar hardness trends could be observed. There was also a hardness fluctuation in the first 120 h ageing, and then the hardness began to increase steadily to a peak value of about 71HV at the 240th hour, followed by an overageing phenomenon. After ageing of 400 h, the hardness remained constant at around 64HV. Further ageing to 1000 h resulted in little change in the hardness. The hardness increase to peak ageing for the Mg-5Sn-1.5Ag alloy was about 10HV (61HV to 71HV) with the increase rate of 16.4%, notably higher than that of the base Mg-5Sn alloy, which had a hardness increment of 4HV and an increase rate of 8%. No clear enhancing effect of Ag on the ageing kinetics was found.

By comparing with the age-hardening response of Mg-5Sn-*x*Ag (x = 0, 0.5, 1, 2) alloys at 200 °C (Ref 11), it could be seen that the ageing kinetics at 160 °C was more sluggish. For all the Mg-Sn-*x*Ag alloys ageing at 200 °C, the hardness exhibited a notable drop in the initial 10 h, and then it started to increase steadily to the peak value after 120 h of ageing (Ref 11). As the ageing temperature decreased to 160 °C, fluctuation of the hardness at the initial ageing stage became evident. The start of the stage of steady hardness increase was postponed to be around 100 h. The peak-aged state was also achieved after 240 h ageing, which is double the time needed for ageing at 200 °C. However, the peak-aged hardness value of the Mg-5Sn-1.5Ag alloy at 160 °C was 71HV, clearly higher than 67.3HV from the peak-aged Mg-5Sn-2Ag alloys. In other words, although the content of Ag decreased, the age-hardening response at 160 °C was more significant. It can be inferred that as the ageing temperature decreases, the diffusion coefficients will decrease exponentially according to diffusion kinetics theories (Ref 17). That is the reason for the more sluggish ageing response of the alloy at 160 °C. On the other hand, a lower ageing temperature indicates more equilibrium precipitates according to Mg-Sn phase diagram (Ref 1) and the possible formation of GP zones at lower ageing temperatures (Ref 18).

It can be seen that 1.5 wt.% addition of Ag significantly improves the age-hardening response of Mg-5Sn alloy at 160 °C. This improvement must result from the microstructure optimizations. To examine the phase constituents of the aged alloys, XRD experiments have been performed on the peak-aged alloys. The XRD patterns of the both alloys are shown in Fig. 3. The indexed patterns show that both the alloys are composed of Mg and Mg_2Sn. In the Mg-5Sn-1.5Ag alloy, though the content of Ag is significant, no clear Ag-containing phase has been detected. This is consistent with the results reported before (Ref 11). It was proposed that Ag mainly forms elemental clusters acting as the heterogeneous nucleation sites for Mg_2Sn precipitates (Ref 16, 11). From the comparison of the two patterns, it can be seen that the peak intensity of Mg_2Sn in the peak-aged Mg-5Sn-1.5Ag alloy is stronger than that in the Mg-5Sn alloy, indicating that the volume fraction of Mg_2Sn in the Mg-5Sn-1.5Ag alloy is larger. In other words, the precipitation process of Mg_2Sn must be enhanced by Ag addition since the ageing time is the same.

The distribution of the precipitates in the peak-aged alloys has been further studied by TEM characterizations, as shown in Fig. 4. The TEM bright-field images of the two alloys are shown in Fig. 4(a) and (c), respectively, with the corresponding diffraction patterns shown in Fig. 4(b) and (d). Both the microstructures were obtained near a $\langle 1\ 1\ -\ 2\ 0 \rangle$ zone axis. In the peak-aged Mg-5Sn alloy, the Mg_2Sn precipitates are distributed sparsely and unevenly in the matrix, while in the Ag-containing alloy, the distribution of the precipitates is much more uniform. In both the alloys, the Mg_2Sn precipitates show a lath morphology lying on the basal plane of the matrix.

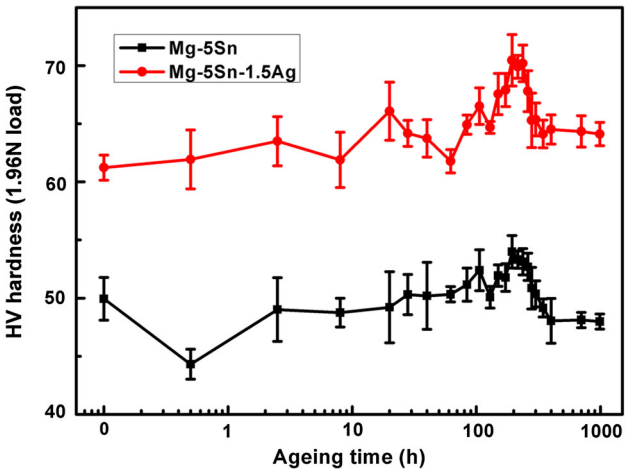

Fig. 2 Age-hardening curves of the Mg-5Sn and Mg-5Sn-1.5Ag alloys subjected to artificial ageing at 160 °C

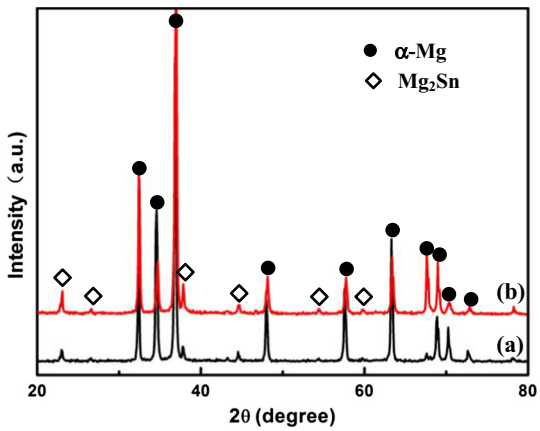

Fig. 3 XRD spectrums of the investigated alloys. (a) Peak-aged Mg-5Sn alloy and (b) peak-aged Mg-5Sn-1.5Ag alloy

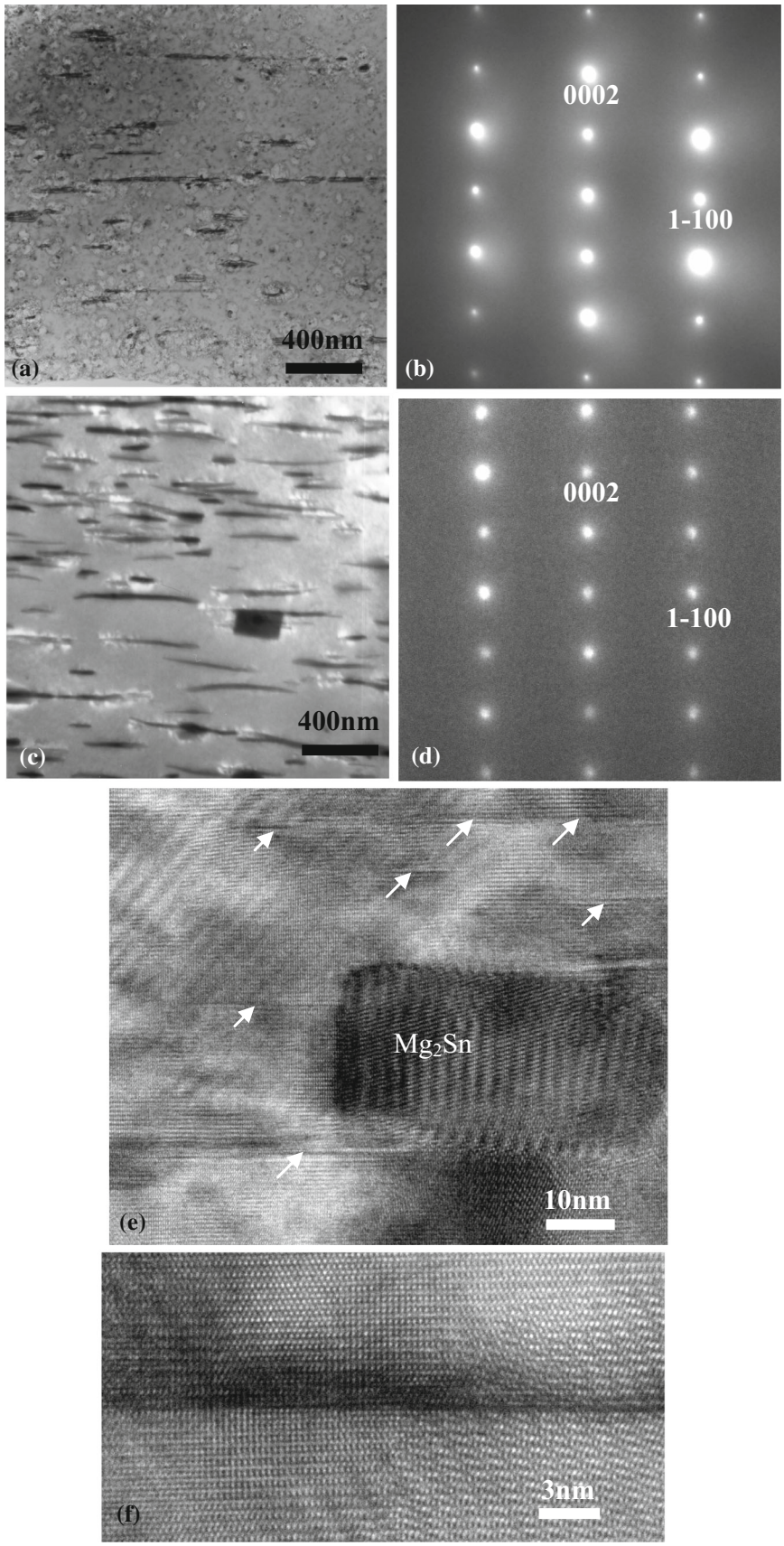

Fig. 4 TEM micrographs of the microstructure from the peak-aged alloys. (a) Bright-field image of the peak-aged Mg-5Sn alloy, (b) SAED pattern corresponding to (a), (c) bright-field image of the peak-aged Mg-5Sn-1.5Ag alloy, (d) SAED pattern corresponding to (c). (e) HRTEM image showing the coexistence of Mg2Sn and the metastable phases indicated by the arrows, (f) HRTEM image of a plate metastable phase

However, the size of Mg_2Sn is significantly refined, and the number density of Mg_2Sn is also clearly improved in the peak-aged Mg-5Sn-1.5Ag alloy. By examining the microstructure thoroughly during TEM observations, the volume fraction of the precipitates in the peak-aged Mg-1.5Sn-0.5Ag alloy is indeed higher. This is consistent with the XRD results in Fig. 3.

Compared with the Mg-5Sn-2Ag alloy aged at 200 °C (Ref 11), it can be found that the peak hardness value is even higher with lower micro-alloying Ag content while the time to peak ageing is retarded. It indicates that the microstructures must be different for ageing at different temperatures. To further examine the precipitates microstructure, a high-resolution transmission electron microscopy (HRTEM) characterization on the microstructure of the peak-aged Mg-5Sn-1.5Ag alloy was conducted. After a careful examination, some plate-like nanosized precipitates were indeed found to be lying on the basal plane of the matrix, as shown in Fig. 4(e) and (f). These thin precipitates have a thickness of only several atoms. The morphology of these plates is the same as the DO_{19} phase found in the Mg-Sn alloy aged at 150 °C (Ref 15). In the present study, this metastable phase exhibits a higher number density than the stable Mg_2Sn precipitates, and it has a nearly coherent interface with the matrix. Usually, these metastable phases are believed to be more effective for precipitation-strengthening alloys (Ref 18). Therefore, it can be inferred that the metastable DO_{19} phase and the stable Mg2Sn have a synergistic strengthening effect for the improved age-hardening response of the Mg-5Sn-1.5Ag alloy at 160 °C.

Figure 5(a) shows the room temperature tensile properties including ultimate tensile strength (UTS), 0.2% proof yield strength (YS), and elongation to fracture of the Mg-5Sn (-1.5)Ag alloys. The mechanical properties were obtained from the average value of three specimens, with the representative stress–strain plots for each alloy at a particular heat-treatment state shown in Fig. 5b. For both the alloys, solid-solution treatment can enhance the strength, and ageing treatment can further improve the strength. In each state, Ag addition improves the strength of the Mg-5Sn alloy. The peak-aged Mg-5Sn-1.5Ag alloy has the maximum UTS of 148 MPa and YS of about 98 MPa. However, the ductility varies in different order for different alloy. As seen from the figure, the Mg-5Sn alloy at the solid solution state has the maximum elongation rate of 11.8%, which is higher than 9.9% at the peak-aged state and 5.2% at the cast state. While for the Mg-5Sn-1.5Ag alloy, the solid-solution treated samples show a higher elongation of 13.9% than the as-cast ones, but the peak-aged alloy obtains the highest elongation of 16.6%.

As seen from the optical microstructure of the cast alloys, the intermetallics are distributed discontinuously along the grain boundaries. These coarse second phases have relatively little effect on yield and tensile strength (Ref 18). In addition, these particles are supposed to crack at small plastic strains to form internal voids, which, under the action of further plastic strain, may coalesce and result in premature fracture (Ref 18); thus, they are detrimental to the ductility. Therefore, the cast alloys show the lowest strength and ductility. When the alloys are solution-treated, although the grain size has increased little, all the alloying elements are dissolved into the matrix, and thus a significant solid-solution strengthening effect can be obtained. Moreover, the single-phase α-Mg solid solution shows better uniform plastic deformation ability than the cast alloys. This is the reason why the solid-solution-treated alloys have better

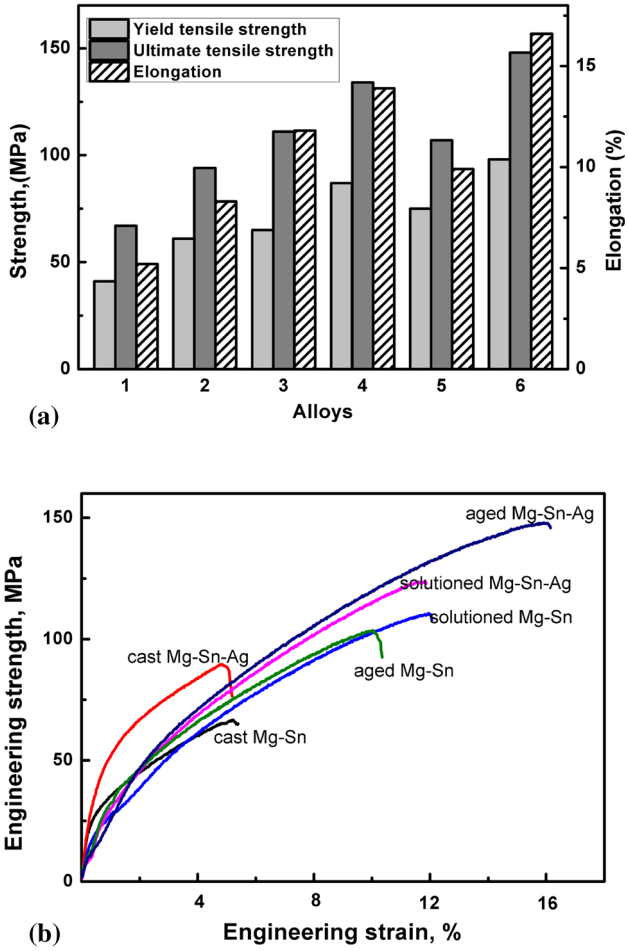

Fig. 5 Tensile properties of the investigated alloys in different states. (a) The designation from '1' to '6' indicates the cast Mg-5Sn alloy, the cast Mg-5Sn-1.5Ag alloy, the solution-treated Mg-5Sn alloy, the solution-treated Mg-5Sn-1.5Ag alloy, the peak-aged Mg-5Sn alloy, and the peak-aged Mg-5Sn-1.5Ag alloy, respectively and (b) representative stress–strain plots of different alloys

strength and ductility than the cast alloys. When the solution-treated alloys were subjected to ageing treatment, dispersively distributed Mg_2Sn precipitates were formed, which produced a remarkable precipitation-strengthening effect, so the peak-aged alloys have the highest yield strengths. However, it is interesting to note that for the peak-aged Mg-5Sn-1.5Ag alloys, the elongation rate is even higher than that at the solid-solution state, which is in contrast to the situation of the Mg-5Sn alloy. Different ductilities of the two peak-aged alloys probably arise from the much different precipitates microstructures. In the peak-aged Mg-5Sn alloy, the coarse Mg_2Sn precipitates may also nucleate microvoids by decohesion at the interface with the matrix which may lead to the formation of sheets of voids (Ref 18), while in the peak-aged Mg-5Sn-1.5Ag alloy, the precipitates have been significantly refined and they can reduce the deformation, and thus toughness is improved.

Figure 6 shows the SEM images of the tensile fracture surfaces for the peak-aged Mg-5Sn and Mg-5Sn-1.5Ag alloys. It can be seen that both the alloys show a characteristic of mixture of quasi-cleavage and ductile fracture, with many distinct dimples and tearing ridges apart from some cleavage steps. However, the dimples in the peak-aged Mg-5Sn-1.5Ag

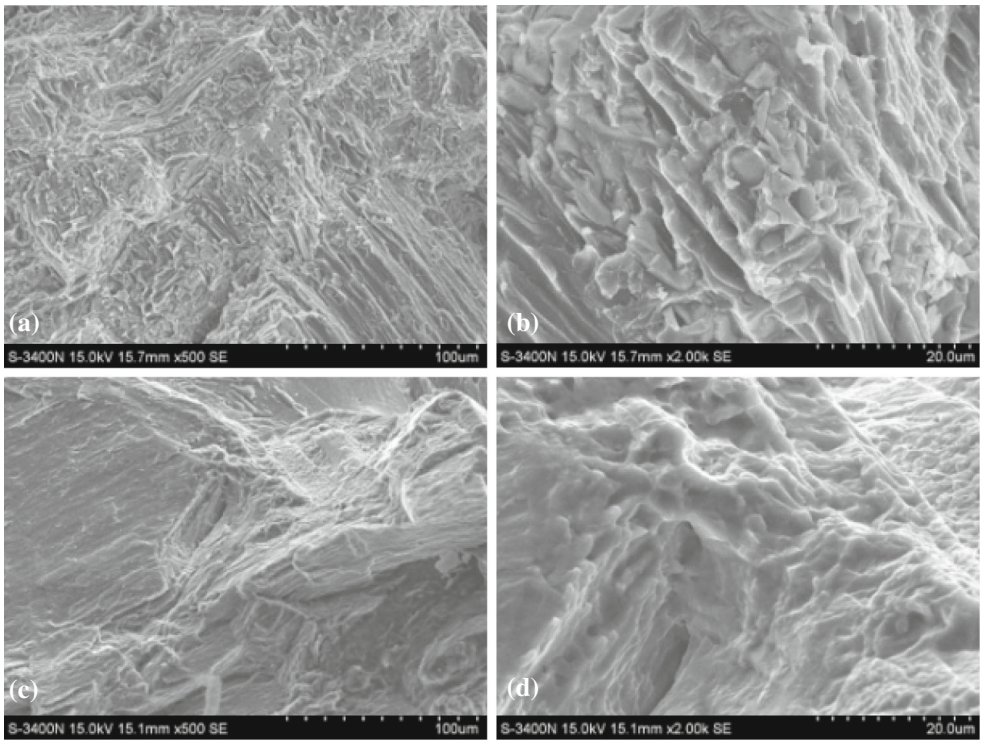

Fig. 6 SEM micrographs showing the fracture surfaces of the aged alloys. (a) and (b) Peak-aged Mg-5Sn alloy, (c) and (d) peak-aged Mg-5Sn-1.5Ag alloy

alloy are more than those in the Mg-5Sn alloy, so the ductility of the Ag-containing alloy is better than that of the base Mg-5Sn alloy. In the peak-aged alloys, there are many precipitates within the matrix. The interfaces between the nanosized precipitates and the matrix probably act as the nucleation sites of the micro-cracks (Ref 19).

4. Conclusions

In summary, the effects of Ag addition and T6 treatment (solid solution + artificial ageing at 160 °C) on the microstructure and mechanical properties of a Mg-5Sn alloy have been investigated, with conclusions drawn as follows:

(1) During the ageing treatment, the hardness of both the Mg-5Sn and Mg-5Sn-1.5Ag alloys exhibits a clear fluctuation in the initial 120 h and then starts to increase steadily. Both the alloys reach the peak-aged state after 240 h ageing, with a peak hardness of 54HV and 71HV, respectively.
(2) Ag addition significantly improves the hardness of the Mg-5Sn alloy at the solid-solution state. The rate of hardness increase caused by ageing has also been improved clearly by Ag additions. These improvements are primarily attributed to the refinement of Mg_2Sn precipitates, the enhanced precipitation process, and the synergistic strengthening effect of Mg_2Sn and a metastable plate DO_{19} phase formed at 160 °C.
(3) Compared to the cast alloys, the solution-treated alloys show a higher yield strength and ductility. Age hardening can further increase the yield strength. The ductility of the Mg-5Sn-1.5Ag alloy is also improved by ageing. Ag addition improves the strength and ductility of Mg-5Sn alloy at each state. The peak-aged Mg-5Sn-1.5Ag alloys exhibit the highest yield strength of 98 MPa and an elongation rate of 16.6%.
(4) The fracture surfaces of the both alloys at the peak-aged state show a characteristic of a mixture of quasi-cleavage and ductile fracture. The fractured surface of the Mg-5Sn-1.5Ag alloy exhibits much more dimples than that of the Mg-5Sn alloy; thus, a better ductility of the Ag-containing alloy is obtained.

Acknowledgments

This research is funded by Chongqing Research Program of Basic Research and Frontier Technology (No. cstc2015jcyjBX0115).

References

1. H. Baker, H. Okamoto, and A.S.M. Handbook, *ASM Handbook Volume 3: Alloy Phase Diagrams*, ASM International, Ohio, 1992
2. M. Bamberger and G. Dehm, Trends in the Development of New Mg Alloys, *Ann. Rev. Mater. Res.*, 2008, **38**, p 505–533
3. J.F. Nie, Precipitation and Hardening in Magnesium Alloys, *Metall. Mater. Trans. A*, 2012, **43A**, p 1–49
4. A.L. Bowles, H. Dieringa, C. Blawert, N. Hort, and K.U. Kainer, Investigations in the Magnesium-Tin System, *Mater. Sci. Forum*, 2005, **488–489**, p 135–138
5. C.L. Mendis, C.J. Bettles, M.A. Gibson, and C.R. Hutchinson, An Enhanced Age Hardening Response in Mg-Sn Based Alloys Containing Zn, *Mater. Sci. Eng. A*, 2006, **435–436**, p 163–171

6. K. Hono, C.L. Mendis, T.T. Sasaki, and K. Oh-ishi, Towards the Development of Heat-Treatable High-Strength Wrought Mg Alloys, *Scripta Mater.*, 2010, **63**, p 710–715
7. T.T. Sasaki, F.R. Elsayed, T. Nakata, T. Ohkubo, S. Kamado, and K. Hono, Strong and Ductile Heat-Treatable Mg-Sn-Zn-Al Wrought Alloys, *Acta Mater.*, 2015, **99**, p 176–186
8. X. Huang, A. Wu, Q. Li, and W. Huang, Effects of Extrusion and Ag, Zn Addition on the Age-Hardening Response and Microstructure of a Mg-7Sn Alloy, *Mater. Sci. Eng. A*, 2016, **661**, p 233–239
9. C.L. Mendis, C.J. Bettles, M.A. Gibson, S. Gorsse, and C.R. Hutchinson, Refinement of Precipitate Distributions in an Age-Hardenable Mg-Sn Alloy Through Microalloying, *Philos. Mag. Lett.*, 2006, **86**, p 443–456
10. T.T. Sasaki, K. Oh-ishi, T. Ohkubo, and K. Hono, Enhanced Age Hardening Response by the Addition of Zn in Mg-Sn Alloys, *Scripta Mater.*, 2006, **55**, p 251–254
11. X. Huang, Y. Du, W. Li, Y. Chai, and W. Huang, Effects of Ag Content on the Solid-Solution and Age-Hardening Behavior of a Mg-5Sn Alloy, *J. Alloy. Compd.*, 2017, **696**, p 850–855
12. X.-F. Huang, W.-Z. Zhang, Y.-S. Ma, and M.-Y. Yin, Enhancement of Hardening and Thermal Resistance of Mg-Sn Based Alloys by Addition of Cu and Al, *Philos. Mag. Lett.*, 2014, **94**, p 460–469
13. S. Behdad, L. Zhou, H.B. Henderson, M.V. Manuel, Y. Sohn, A. Agarwal, and B. Boesl, Improvement of Aging Kinetics and Precipitate Size Refinement in Mg-Sn Alloys by Hafnium Additions, *Mater. Sci. Eng. A*, 2016, **651**, p 854–858
14. X.-F. Huang and W.-Z. Zhang, Improved Age-Hardening Behavior of Mg-Sn-Mn Alloy by Addition of Ag and Zn, *Mater. Sci. Eng. A*, 2012, **552**, p 211–221
15. Y.K. Kim, D.H. Kim, W.T. Kim, and D.H. Kim, Precipitation of DO_{19} Type Metastable Phase in Mg-Sn Alloy, *Mater. Lett.*, 2013, **113**, p 50–53
16. C.Q. Liu, H.W. Chen, H. Liu, X.J. Zhao, and J.F. Nie, Metastable Precipitate Phases in Mg-9.8 wt%Sn Alloy, *Acta Mater.*, 2018, **144**, p 590–600
17. B.-C. Zhou, S.-L. Shang, Y. Wang, and Z.-K. Liu, Diffusion Coefficients of Alloying Elements in Dilute Mg Alloys: A Comprehensive First-Principles Study, *Acta Mater.*, 2016, **103**, p 573–586
18. I.J. Polmear, *Light Alloys*, 4th ed., Elsevier Butterworth-Heinemann, Oxford, 2006
19. H.-M. Zhu, C.-P. Luo, J.-W. Liu, and D.-L. Jiao, Effects of Cu Addition on Microstructure and Mechanical Properties of As-Cast Magnesium Alloy ZK60, *Trans. Nonferrous Metal Soc.*, 2014, **24**, p 605–610